eor.istanbul.edu.tr

Official Publication of Istanbul University Faculty of Dentistry

Eur Oral Res 2025; 59(2): 138-143

Original research

Finite element analysis of stresses on the skull base caused by trauma during sinus lift with mallet and osteotome

Alparslan Esen[1], **Çağrı Esen**[2]

Purpose
This study aimed to investigate the stress accumulation on the skull base caused by the forces applied to fracture the bone at the sinus floor during the closed trans-alveolar technique of sinus elevation.

Materials and Methods
This study was based on three-dimensional finite element analysis. Study models were determined as follows: Model 1, Model 2, and Model 3 (bone thickness at the sinus floor 1, 2, and 3 mm, respectively). The forces required for fracture of the bone at the base of the sinus were found to be 89,04 N, 138,88 N, and 210 N for Models 1, 2, and 3, respectively. The von Mises (VM), maximum principal (Pmax), and minimum principal (Pmin) stress values were examined at three different locations in the petrous part of the temporal bone. The highest stress values during the fracture process were recorded.

Results
During fracture, VM, Pmax, and Pmin stress values were highest in Model 3 and lowest in Model 1. When the most critical levels were analyzed, it was seen that all stress values in Model 3 were more than twice the values in Model 1.

Conclusion
In closed trans-alveolar sinus lifting, as the forces applied to break the bone at the sinus floor increase, the stress accumulation at the petrous part of the temporal bone increases in direct proportion. This increase in cranial base stress may lead to an increased risk of benign paroxysmal positional vertigo which is a major complication of closed sinus lifting.

Keywords: *Benign paroxysmal positional vertigo, finite element analysis, sinus lifting, mallet, osteotome*

Introduction

The posterior maxilla is a challenging area for implant placement when there is insufficient bone. The most common causes of bone insufficiency in this region are bone resorption after tooth extraction, advanced periodontal disease, and pneumatization of the maxillary sinus. Sinus lifting or augmentation is a routine procedure when there is insufficient vertical bone for implant placement in the posterior maxilla. Currently, there are two widely used techniques for maxillary sinus augmentation: the open lateral window (OLW) technique and the closed transalveolar (CTA) technique. In the CTA technique, also known as the osteotome or transcrestal technique, the sinus floor is elevated by hitting an osteotome with a mallet. Previous studies have reported that implant placement with the CTA technique is a highly predictable treatment option (1,2). The CTA technique is preferred as an alternative to the OLW technique in sinus floor elevation when the bone height is within vertical limits (5-7 mm) (3). It is less invasive than the OLW technique, has a shorter operative time, and causes less postoperative discomfort (4). How-

ORCID IDs of the authors: A.E. 0000-0001-7419-3210; C.E. 0000-0002-4358-1293

[1]*Department of Oral and Maxillofacial Surgery, Faculty of Dentistry, Necmettin Erbakan University, Konya, Türkiye*

[2]*Department of Periodontology, Faculty of Dentistry, Nevşehir Hacı Bektaş Veli University, Nevşehir, Türkiye*

Corresponding Author: Çağrı Esen

E-mail: cagriesen@hotmail.com

Received: 18 February 2024
Revised: 20 March 2024
Accepted: 24 April 2024

DOI: 10.26650/eor.20241439180

How to cite: *Esen A, Esen Ç. Finite element analysis of stresses on the skull base caused by trauma during sinus lift with mallet and osteotome. Eur Oral Res 2025; 59(2): 138-143.* DOI: 10.26650/eor.20241439180

ever, like any surgical procedure, CTA sinus lifting has various complications. The most common complication is the rupture of the sinus membrane, similar to the OLW technique. Other major complications include infection, bleeding, sinusitis, and benign paroxysmal positional vertigo (BPPV) (5).

Benign paroxysmal positional vertigo (BPPV) is characterized by short and recurrent vertigo attacks triggered by changes in head position relative to gravity. BPPV occurs when otoliths, which are calcium carbonate crystals, leave the utricle and migrate into the lumen of the semicircular canals (6). The semicircular canals and utricles, which are elements of the vestibular system, are located in the membranous labyrinth filled with endolymph fluid. The membranous labyrinth is surrounded by the otic capsule or osseous labyrinth. All these inner ear structures lie deep within the petrous part of the temporal bone (7). The etiology of BPPV is sometimes unclear. The most common type of BPPV is the idiopathic form, which occurs without a specific cause. The type that occurs after factors such as head trauma, neck injury, or head and neck surgery is called secondary BPPV (8). The trauma caused by the mallet and osteotome used in the CTA technique of sinus elevation may also be one of the effective factors in the formation of BPPV (9).

The purpose of this study was to assess the stress distribution at the petrous part of the temporal bone, where the otoliths dislodge from the utricle of the inner ear and move within the lumen of the semicircular canals. We hypothesized that as the bone thickness left at the sinus floor increases, the stresses on the skull base will also increase during the procedure. The specific aim of this study was to experimentally determine whether sinus lifting could be a risk factor for BPPV.

Materials and Methods

Study design

This study is based on three-dimensional finite element analysis. Study models were determined as follows: Model 1 (bone thickness at the sinus floor 1 mm), Model 2 (2 mm), and Model 3 (3 mm). The first molar region at the maxilla was chosen as the load-applied region to fracture the bone at the base of the sinus (Figure 1). The forces required to break the bone left at the sinus floor with a thickness of 1, 2, and 3 mm (Model 1, 2, and 3) were determined as 89.04 N, 138.88 N, and 210 N, respectively. With gradually applied forces, bone fracture times for Models 1, 2, and 3 were determined as 2.5, 2.95, and 5.2 milliseconds, respectively. Von Mises (VM), maximum principal (Pmax), and minimum principal (Pmin) stresses were measured at three different locations in the petrous part of the temporal bone (Figure 2). Arranging the three-dimensional mesh structure and transforming it into a mathematically appropriate solid mesh structure, creating three-dimensional finite element analysis models, and finite element stress analysis were performed on workstations (HP Inc., California, USA) with a processor (Intel Corporation, California, USA) at 2.40 GHz and 64 GB memory.

The bone models

The bone model in .stl format was obtained from tomography data using software (3D Slicer, https://www.slicer.org/) (10). Reverse engineering and three-dimensional CAD processes were carried out using the same software (Ansys SpaceClaim, Ansys, Inc., USA). The activities of adapting the solid models to the analysis environment and creating the optimized mesh were carried out with another software (Ansys LS-DYNA, Ansys, Inc., USA).

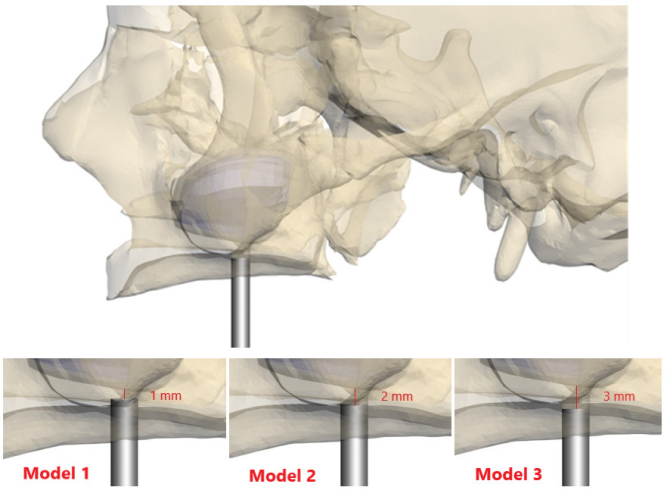

Figure 1. *The first molar region at the maxilla was chosen as the load-applied region to fracture the bone at the base of the sinus. Loads were applied to break the bone left at the base of the sinus with a thickness of 1 mm (Model 1), 2 mm (Model 2), and 3 mm (Model 3).*

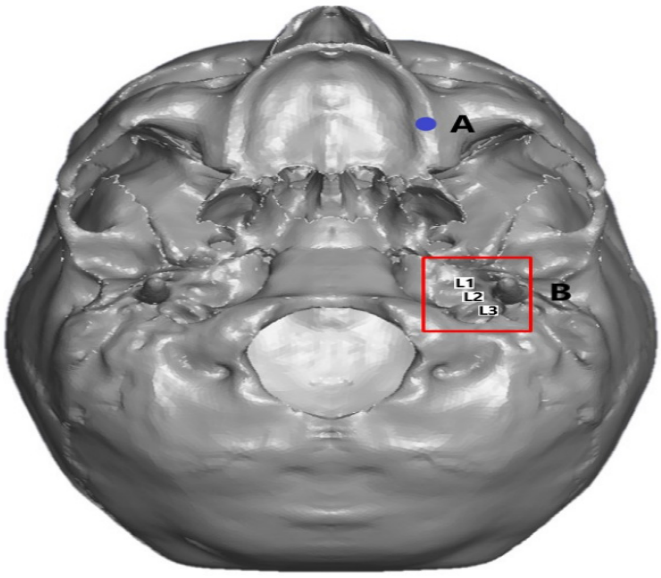

Figure 2. *The blue circular region (A) on the inferior view of the skull base represents the location of the osteotome applied on the maxillary crest. The red frame (B) represents the petrous part of the temporal bone. L1, L2, and L3 indicate the areas where stress values are determined.*

Modeling of cortical and trabecular bone

To create the maxillary bone model used in the study, a computed tomography (CT) scan of an edentulous adult individual was taken. CT data were reconstructed with a slice thickness of 0.1 mm. The CT data obtained from the reconstruction were transferred to software (3D Slicer, https://www.

slicer.org/) in DICOM format. The CT data in DICOM format were separated according to the appropriate Hounsfield values and converted into three-dimensional models through segmentation. Models were exported in .stl format. The modeling process was completed by placing all prepared models in the correct coordinates in three-dimensional space with the software (Ansys SpaceClaim, Ansys, Inc., USA).

Obtaining mathematical models

Mathematical models were created by dividing geometric models into small and simple parts called meshes. Once the modeling process was completed, the models were created mathematically and made ready for analysis. In the analysis study, time-dependent dynamic simulations were carried out. The explicit analysis method was used to model short-term and dynamic loads and examine their effects on the structure. In the finite element model setup, 1 mm was chosen as the average element size, and the models consisted of approximately 3 million elements and 600,000 nodal points. All parts were modeled using solid elements, and the Lagrange approach was used.

Material definitions and properties

Isotropic elastic-rubber material properties of the given materials were used while determining the elastic modulus, Poisson's ratio, and density in the analyses. The material properties of the analyzed model were defined numerically (Table 1). The total node and element amounts used in the models are shown in Table 2. The MAT_ELASTIC material model was used to model the skull.

Loading scenarios and boundary conditions

In the analysis model, no boundary conditions were applied in order not to cause an undesirable strain on the skull. Different loads were applied vertically to the bone at the base of the maxillary sinus by means of the impactor piece which simulates the osteotome and thus the fracture was ensured to occur in the load region. Iterative simulations were carried out in order to find the load that causes fracture in the bone. The force definition in the analysis model was performed with the LOAD_NODE_SET definition in the software (Ansys LS-DYNA, Ansys, Inc., USA). The breaking load was determined by defining different force values for the nodal point group formed on the bottom surface of the impactor part. The iterative analysis solutions calculated the force value that creates the fracture behavior in bone structures of different thicknesses.

Table 1. *The material properties of the analyzed model.*

Material	Elastic Modulus (MPa)	Poisson's Ratio *v*	Density (kg/m3)
Skull Bone	8000	0.22	1200

MPa, megapascal; kg/m³, kilogram/cubic meter.

Table 2. *Quantitative model information for the three analysis models created.*

	Total Number of Nodes	Total Number of Elements
Model 1	603035	3010613
Model 2	604270	3018228
Model 3	603933	3015622

Results

The VM, Pmax, and Pmin stress were evaluated at three different locations (L1, L2, and L3) of the petrous part of the temporal bone (Figure 3). The values where VM, Pmax, and Pmin stresses reached the highest level during the fracture process were determined (Table 3). Accordingly, the highest stress values at the petrous part of the temporal bone were

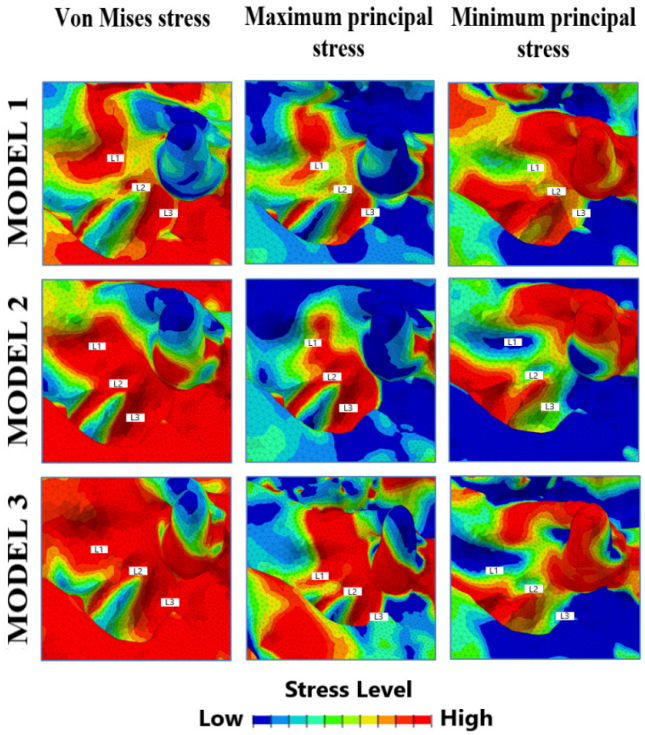

Figure 3. *The von Mises stress, maximum principal stress, and minimum principal stress levels in Models 1, 2, and 3 are shown with colored stress plots. The L1, L2, and L3 regions indicated on the colored stress plots show three different locations where the stress values were determined at the petrous part. It is seen that the stress levels increase from Model 1 to Model 2 and Model 3.*

Table 3. *The VM, Pmax, and Pmin stress values reached the most critical levels during the fracture process at different locations (L1, L2, and L3) on the cranial base.*

		Model 1	Model 2	Model 3
VM stress (Mpa)	**L1**	1.23	1.89	2.83
	L2	1.03	1.53	2.49
	L3	1.15	1.37	4.42
Pmax stress (Mpa)	**L1**	0.85	1.11	1.97
	L2	0.75	0.96	1.73
	L3	0.99	1.18	4.16
Pmin stress (Mpa)	**L1**	-0.61	-1.30	-1.52
	L2	-0.58	-0.90	-1.66
	L3	-0.39	-0.41	-1.48

observed in Model 3. The order of the stress values according to the models is Model 3 > Model 2 > Model 1.

Discussion

In this study, our purpose was to investigate the stress accumulation on the skull base caused by the forces applied to break the bone at the sinus floor during the CTA technique sinus elevation using a mallet and osteotome. We aimed to evaluate the stress distribution generated by the osteotome and mallet on the petrous part of the temporal bone, where BPPV occurs. We determined study models based on the thickness of the bone left to fracture at the sinus floor (Models 1, 2, and 3; 1 mm, 2 mm, and 3 mm, respectively). During the fracture process, as the thickness of the fractured bone at the base of the maxillary sinus increased, the most critical levels of VM stress, Pmax stress, and Pmin stress increased at all locations of the petrous portion. These stress increases were more than double in Model 3 compared to Model 1 at all locations, while they were more than quadrupled in some locations. Therefore, at the petrous region, it appears that the tension and compression increase due to the increase in Pmax and Pmin stresses, and sensitivity occurs due to the increase in VM stress.

There are many BPPV cases reported after maxillofacial procedures using osteotome and mallet in the literature. Most of these reported cases of BPPV after osteotome and mallet use are sinus elevation procedures performed with the closed technique (9, 11-15). Other maxillofacial procedures reported for BPPV after osteotome and mallet use include buccolingual widenings of narrow alveoli before implant placement (16, 17), LeFort osteotomy (18, 19), and wide carcinoma resection (20). Some authors have also reported cases of BPPV after wisdom tooth extractions and open sinus augmentation with implant placement (21-24). These authors attributed the cause of BPPV to prolonged head and neck hyperextension during the operation or to the vibration created by rotary instruments and burs used. However, a controlled clinical study on this subject showed that the use of mallet and osteotome was more prominent in the occurrence of BPPV than other factors (9). The results of another study also supported this finding (14).

Although cases of BPPV occurring after CTA sinus elevation have been reported, to the best of our knowledge, there is no study in the literature on the determination of the strength and stress values created by the osteotome and mallet. In this study, we aimed to determine the forces required to break the bone at the sinus floor during CTA sinus elevation and to determine the stress reflections of these forces at the petrous part of the temporal bone where BPPV occurs.

Summers (25), in describing the osteotome technique in 1994, reported that both the implant bed could be formed and the sinus floor could be raised with only the osteotome and mallet, without using rotary instruments. However, Misch et al. (26) later recommended creating an implant bed 1-2 mm below the sinus floor with rotary instruments and drills, and then breaking this bone into the sinus with an osteotome and mallet. On the other hand, Klokkevold et al. (27) stated that this bone thickness under the sinus floor can be left at 2-3 mm, while others (3) reported that it should be drilled up to the sinus floor without leaving any bone at the sinus floor. In summary, there is no complete consensus on this issue. In this study, we wanted to evaluate 1, 2, and 3 mm, which are more frequently used by clinicians and are compatible with the literature. Despite clinical and radiographic evaluations, clinicians rarely have difficulty breaking the bone at the base of the maxillary sinus during sinus elevation with the CTA technique. The reasons for this situation may be variations in the anatomy of the sinus floor, miscalculations made in X-ray images, and overly protective approaches to prevent rupture of the Schneiderian membrane during surgery.

When the forces occurring at the time of bone fracture at the sinus floor were examined, it was observed that a significant increase in strength occurred for every 1 mm increase in bone thickness. When the thickness of the bone at the sinus floor was increased from 1 mm to 2 mm, an additional force of approximately 50 N was required to break this bone. When the thickness of this bone was increased from 2 mm to 3 mm, an additional force of approximately 70 N was required.

The petrous part of the temporal bone represents the hard tissues in which the inner ear elements responsible for the vestibular system are located (7). BPPV occurs when otoliths dislodge from the utricle of the inner ear and move within the lumen of the semicircular canals (6). Considering the stresses at the petrous part of the temporal bone as a potential cause of BPPV, we believe that the thickness of the fractured bone at the sinus floor is very important. Clinically, if thick bone is left at the base of the sinus, more force will be required to break this bone. Accordingly, the tension, compression stresses, and sensitivity at the skull base will increase. In this case, it can be considered that the risk of BPPV will increase.

In this experimental study, the dynamic loading approach was used instead of static loading, which is generally applied in finite element analysis studies in the field of maxillofacial surgery. Thus, a better representation of osteotome movement is provided. Instead of evaluating the stress at the moment of loading as in static loading, we had the chance to determine the moment of bone fracture and evaluate the most critical stress levels up to that moment. In addition, we considered the plastic material properties of the bone as well as the elastic material properties while creating the bone model. Thus, the moment of fracture is simulated more realistically.

Conclusion

Within the limits of this study, we showed that during the CTA sinus elevation procedure using an osteotome and mallet, the stresses on the temporal bone increase dramatically and disproportionately with each 1 mm increase in the bone to be broken at the base of the sinus. This stress increase at the cranial base may lead to an increased risk of BPPV. Considering these data, clinicians need to be aware of BPPV, which causes symptoms that reduce the patient's quality of life. We think that to avoid BPPV, they should perform a detailed radiographic analysis before the CTA technique and pay attention to the forces applied during this procedure.

Türkçe öz: *Çekiç ve osteotom ile sinüs yükseltme sırasında meydana gelen travmanın kafatası tabanında oluşturduğu streslerin sonlu elemanlar analizi. Amaç: Bu çalışmada kapalı trans-alveolar sinüs yükseltme tekniği sırasında sinüs tabanında bırakılan kemiğin kırılmasına yönelik uygulanan kuvvetlerin kafa tabanında neden olduğu stres birikiminin araştırılması amaçlandı. Gereç ve yöntem: Bu çalışma üç boyutlu sonlu elemanlar analizine dayanmaktadır. Çalışma modelleri şu şekilde belirlendi: Model 1, Model 2 ve Model 3 (sinüs tabanındaki kemik kalınlığı sırasıyla 1, 2 ve 3 mm). Sinüs tabanındaki kemiğin kırılması için gerekli kuvvetler Model 1, 2 ve 3 için sırasıyla 89,04 N, 138,88 N ve 210 N olarak tespit edildi. Von Mises (VM), maksimum asal (Pmax) ve minimum asal (Pmin) stres değerleri, temporal kemiğin petröz kısmında üç farklı lokasyonda incelenmiştir. Kırılma sürecindeki en yüksek stres değerleri kaydedildi. Bulgular: Kırılma sırasında VM, Pmax ve Pmin stres değerleri Model 3'te en yüksek, Model 1'de en düşüktü. En kritik seviyeler incelendiğinde Model 3'teki tüm stres değerlerinin Model 1'deki değerlerin iki katından fazla olduğu görüldü. Sonuç: Kapalı trans-alveoler sinüs yükseltme işleminde sinüs tabanındaki kemiği kırmak için uygulanan kuvvetler arttıkça temporal kemiğin petröz kısmındaki stres birikimi de doğru orantılı olarak artar. Kranial taban stresindeki bu artış, kapalı sinüs kaldırmanın önemli bir komplikasyonu olan benign paroksismal pozisyonel vertigo riskinin artmasına yol açabilir. Anahtar Kelimeler: benign paroksismal pozisyonel vertigo, sonlu elemanlar analizi, sinüs yükseltme, çekiç osteotom*

Ethics Committee Approval: None

Informed Consent: Participants provided informed constent.

Peer-review: Externally peer-reviewed.

Author contributions: AE and CE participated in designing the study. AE and CE participated in generating the data for the study. AE and CE participated in gathering the data for the study. AE and CE participated in the analysis of the data. AE wrote the majority of the original draft of the paper. CE participated in writing the paper. AE and CE have had access to all of the raw data of the study. AE has reviewed the pertinent raw data on which the results and conclusions of this study are based. AE and CE have approved the final version of this paper. CE guarantees that all individuals who meet the Journal's authorship criteria are included as authors of this paper.

Conflict of Interest: The authors declared that they have no conflict of interest.

Financial Disclosure: This work was supported by the Necmettin Erbakan University Research Fund Grant [Project number: 211224006].

Acknowledgments: The authors would like to thank Kaan Yardimci (Mechanical Engineer) and Tinus Technologies for their contributions and support.

References

1. Nedir R, Nurdin N, Vazquez L, Abi Najm S, Bischof M. Osteotome Sinus Floor Elevation without Grafting: A 10-Year Prospective Study. Clin Implant Dent Relat Res 2016;18:609-17. doi: 10.1111/cid.12331. [CrossRef]
2. Chen MH, Shi JY. Clinical and Radiological Outcomes of Implants in Osteotome Sinus Floor Elevation with and without Grafting: A Systematic Review and a Meta-Analysis. J Prosthodont 2018;27:394-401. doi: 10.1111/jopr.12576. [CrossRef]
3. Lundgren S, Cricchio G, Hallman M, Jungner M, Rasmusson L, Sennerby L. Sinus floor elevation procedures to enable implant placement and integration: techniques, biological aspects and clinical outcomes. Periodontol 2000 2017;73:103-20. doi: 10.1111/prd.12165. [CrossRef]
4. Emmerich D, Att W, Stappert C. Sinus floor elevation using osteotomes: a systematic review and meta-analysis. J Periodontol 2005;76:1237-51. doi: 10.1902/jop.2005.76.8.1237. [CrossRef]
5. Saker M, Ogle O. Benign paroxysmal positional vertigo subsequent to sinus lift via closed technique. J Oral Maxillofac Surg 2005;63:1385-7. doi: 10.1016/j.joms.2005.05.296. [CrossRef]
6. Fife TD. Benign paroxysmal positional vertigo. Semin Neurol 2009;29:500-8. doi: 10.1055/s-0029-1241041. [CrossRef]
7. Cole SR, Honaker JA. Benign paroxysmal positional vertigo: Effective diagnosis and treatment. Cleve Clin J Med 2022;89:653-62. doi: 10.3949/ccjm.89a.21057.
8. Chen G, Li Y, Si J, Zhao X, Zhang T, Dai X, Yu G. Treatment and recurrence of traumatic versus idiopathic benign paroxysmal positional vertigo: a meta-analysis. Acta Otolaryngol 2019;139:727-33. doi: 10.1080/00016489.2019.1632484. [CrossRef]
9. Sammartino G, Mariniello M, Scaravilli MS. Benign paroxysmal positional vertigo following closed sinus floor elevation procedure: mallet osteotomes vs. screwable osteotomes. A triple blind randomized controlled trial. Clin Oral Implants Res 2011;22:669-72. doi: 10.1111/j.1600-0501.2010.01998.x. [CrossRef]
10. Fedorov A, Beichel R, Kalpathy-Cramer J, Finet J, Fillion-Robin JC, Pujol S, Bauer C, Jennings D, Fennessy F, Sonka M, Buatti J, Aylward S, Miller JV, Pieper S, Kikinis R. 3D Slicer as an image computing platform for the Quantitative Imaging Network. Magn Reson Imaging 2012;30:1323-41. doi: 10.1016/j.mri.2012.05.001. [CrossRef]
11. Di Girolamo M, Napolitano B, Arullani CA, Bruno E, Di Girolamo S. Paroxysmal positional vertigo as a complication of osteotome sinus floor elevation. Eur Arch Otorhinolaryngol 2005;262:631-3. doi: 10.1007/s00405-004-0879-9. [CrossRef]
12. Su GN, Tai PW, Su PT, Chien HH. Protracted benign paroxysmal positional vertigo following osteotome sinus floor elevation: a case report. Int J Oral Maxillofac Implants 2008;23:955-9.
13. Vernamonte S, Mauro V, Vernamonte S, Messina AM. An unusual complication of osteotome sinus floor elevation: benign paroxysmal positional vertigo. Int J Oral Maxillofac Surg 2011;40:216-8. doi: 10.1016/j.ijom.2010.07.010. [CrossRef]
14. Al-Almaie S, Kavarodi AM, Al Faidhi A. Maxillary sinus functions and complications with lateral window and osteotome sinus floor elevation procedures followed by dental implants placement: a retrospective study in 60 patients. J Contemp Dent Pract 2013;14: 405-13. doi: 10.5005/jp-journals-10024-1336. [CrossRef]
15. Akcay H, Ulu M, Kelebek S, Aladag I. Benign Paroxysmal Positional Vertigo Following Sinus Floor Elevation in Patient with Antecedents of Vertigo. J Maxillofac Oral Surg 2016;15:351-4. doi: 10.1007/s12663-016-0891-9. [CrossRef]
16. Peñarrocha M, Pérez H, Garciá A, Guarinos J. Benign paroxysmal positional vertigo as a complication of osteotome expansion of the maxillary alveolar ridge. J Oral Maxillofac Surg 2001;59:106-7. doi: 10.1053/joms.2001.19307. [CrossRef]
17. Kaplan DM, Slovik Y, Joshua BZ, Puterman M, Kraus M. Head shaking during Dix-Hallpike exam increases the diagnostic yield of posterior semicircular canal BPPV. Otol Neurotol 2013;34:1444-7. doi: 10.1097/MAO.0b013e3182953120. [CrossRef]
18. Beshkar M, Hasheminasab M, Mohammadi F. Benign paroxysmal positional vertigo as a complication of orthognathic surgery. J Craniomaxillofac Surg 2013;41:59-61. doi: 10.1016/j.jcms.2012.05.012. [CrossRef]
19. Deniz K, Akdeniz SS, Koç AÖ, Uckan S, Ozluoğlu LN. Evaluation of benign paroxysmal positional vertigo following Le Fort I osteotomy. Int J Oral Maxillofac Surg 2017;46:309-13. doi: 10.1016/j.ijom.2016.10.007. [CrossRef]
20. Nigam A, Moffat DA, Varley EW. Benign paroxysmal positional vertigo resulting from surgical trauma. J Laryngol Otol 1989;103:203-4. doi: 10.1017/s0022215100108448. [CrossRef]

21. Rodríguez Gutiérrez C, Rodríguez Gómez E. Positional vertigo afterwards maxillary dental implant surgery with bone regeneration. Med Oral Patol Oral Cir Bucal 2007;12:151-3.
22. D'Ascanio L, Salvinelli F, Martinelli M. Benign paroxysmal positional vertigo: an unusual complication of molar teeth extraction. Br J Oral Maxillofac Surg 2007;45:176-7. doi: 10.1016/j.bjoms.2006.03.003. [CrossRef]
23. Chiarella G, Leopardi G, De Fazio L, Chiarella R, Cassandro E. Benign paroxysmal positional vertigo after dental surgery. Eur Arch Otorhinolaryngol 2008;265:119-22. doi: 10.1007/s00405-007-0397-7. [CrossRef]
24. Reddy K S, Shivu ME, Billimaga A. Benign paroxysmal positional vertigo during lateral window sinus lift procedure: a case report and review. Implant Dent 2015;24:106-9. doi: 10.1097/ID.0000000000000188. [CrossRef]
25. Summers RB. A new concept in maxillary implant surgery: the osteotome technique. Compendium 1994;15:152-62.
26. Misch CE., Resnik RR, Misch-Dietsh, F. Maxillary sinus anatomy, pathology and graft surgery. IN: Mish CE, ed. Contemporary Implant Dentistry. 3rd ed. Mosby Elsevier 2008:905-74.
27. Klokkevold PR, Urban IA, Cochran DL. Advanced Implant Surgical Procedures. IN: Newman MG, Takei H, Klokkevold PR, Carranza FA, eds. Carranza's Clinical Periodontology. 11th ed. Saunders Elsevier 2011:684-94. [CrossRef]